J. Cosmet. Sci., 69, 121–130 (March/April 2018)

Structural Analysis of Macrofibrils in a Human Permanent Waved Hair by Scanning Microbeam Small-Angle X-ray Scattering Measurements

MAKI FUKUDA, YUKI MARUBASHI, TEPPEI NAWA, and REINA IKUYAMA, *Beauty Care Laboratory, Kracie Home Products, Ltd., Yokohama 240-0005, Japan (M.F., R.I.), General Research & Development Institute, Hoyu Co., Ltd., Nagakute 480-1136, Japan (Y.M., T.N.)*

Accepted for publication March 27, 2018.

Synopsis

It has been experimentally shown that hair subjected to permanent wave treatment quickly changes into uncurled hair during daily hair-care activities. However, the mechanism of curl fallout has not been clarified. In previous studies, the relationship between permanent wave treatment and disulfide bonds in hair has been studied. Because permed hair falls out its waves without any chemical treatment, we focused on the hair microstructure rather than the disulfide bonds. To examine the relationship between the hair curl shape and the intermediate filament (IF) organization in hairs, scanning microbeam small-angle X-ray scattering measurements were performed. It was found that in permed hairs, the IF orientation on the convex side of the curvature was different from that on the concave side. By contrast, for permed hairs with curl fallout, the IF orientation on the convex curvature side was not significantly different from that on the concave side. Our findings suggest that the curl shape of permed hairs is related to its anisotropic IF orientation between the convex and concave side of the curl, and control of this IF orientation will allow for effective reduction of curl fallout.

INTRODUCTION

A permanent wave (perm) can produce a hairstyle of one's choice, and is familiar to people around the world. Basically, the perm treatment consists of two processes. In the first process, the hair is wrapped around perm rods, and is treated with a reducing agent such as thioglycolic acid. These agent molecules break some of the disulfide cross-links between polypeptide bonds in keratin, a protein present in hair. In the second process, the hair is treated with oxidizing agents while it is still wrapped around the rods. These agents reform the previously broken disulfide bonds, but in such a way that it stabilizes the hair in their position around the rod. As a result, the hair exhibits waves even when the rods are removed. Disulfide bonds in hair are, thus, central in these processes, and their role in permanent wave treatments has, therefore, been extensively studied (1–5).

Address all correspondence to Teppei Nawa at teppei_nawa@hoyu.co.jp.

However, many of these studies have dealt with the effect of permanent wave treatment on hair that was not wrapped around perm rods. For this reason, the relationship between hair curl shapes and disulfide bonds may not have been fully understood. One factor is curl fallout: Curl fallout is the phenomenon by which, through daily hair care, the waves formed through perm treatment begin to deteriorate after roughly 1 mo. Although this issue of hairstyle maintenance poses problems to many, this phenomenon has not been studied, and the cause of curl fallout has not yet been clarified. Because permed hair falls out its waves without any chemical treatment, we investigated changes in the microstructure of the hair rather than in disulfide bonds.

Because of recent developments of scanning microbeam small angle X-ray scattering (SAXS) technology, it is now possible to examine the inner microstructures of hair (6–11). The relationship between the shape of hair curls in naturally curly hair and the orientation of intermediate filaments (IFs) in the hair could, thus, be explored (12). The present study aims to clarify the cause of curl fallout, by investigating the relationship between the IF's orientation and the curl shape of permed hair. To investigate the relationship, five types of hair samples were prepared. The first samples were hairs without perm treatment. The second samples were permed hair. The third samples were permed hairs repeatedly stretched. The forth samples were permed hair immersed sodium lauryl sulphate (SLS) solution. The Last samples were permed hairs stretched and immersed SLS solution. These samples were examined by scanning microbeam SAXS for structural analysis, and the relationship between curl shape and microstructure was discussed.

MATERIALS AND METHODS

CURL DIAMETER EFFICIENCY MEASUREMENTS

Asian blended untreated hairs were used. Each hair bundle curl diameter was measured in a room where the temperature and humidity were adjusted to 25°C and 50% Relative Humidity (RH), respectively.

The "curl diameter efficiency" was calculated using the formula:

$$\text{Curl diameter efficiency (\%)} = \text{Rod diameter (mm)}/\text{Curl diameter (mm)} \times 100.$$

Fifteen millimeter diameter spiral rods were used. The curl diameter efficiency was determined after the perm treatment and after each subsequent treatment (described in the following text). Each treatment was performed five times, and average data was used for analysis.

CHEMICAL TREATMENTS FOR CURL DIAMETER EFFICIENCY MEASUREMENTS

Bleached hair. A bleach treatment was carried out for 35 min at 30°C using 1.0 wt% ammonia aq. and 3.0 wt% hydrogen peroxide aq. (pH 10.2) (⇒ bleached hairs). The scale of curl fallout was not sufficiently large in virgin hairs after only a perm treatment to get reliable results. Hairs were, therefore, first bleached and then permed, making the measured differences more prominent. We used bleached hairs as a control.

Permed hair. Bleached hairs were wrapped around a 15-mm-diameter spiral rod, and were treated for 15 min at 30°C using 6.0 wt% thioglycolic acid aq. and 0.8 wt% ammonia aq. (pH 9.4). After washing with water, the hairs were treated for 15 min at 30°C using 7.0 wt% sodium bromate aq. (pH 6.9) (⇒ permed hairs).

Stretched hairs. The permed hairs were combed through five times. This treatment was repeated 30 times.

SLS-immersed hair. The permed hairs were immersed in 5.0 wt% SLS aq. (pH 8.5) for 3 min. This subsequent treatment was repeated 30 times.

Stretched SLS-immersed hair. The permed hairs were immersed in 5.0 wt% SLS aq. (pH 8.5) for 3 min. After immersing the hairs in water for 2 min, they were combed through five times. This subsequent treatment was repeated 30 times.

SAXS MEASUREMENTS

Asian untreated hairs, with a diameter of 70–90 μm, from a single head were used. In addition, naturally curly hairs were excluded and only straight hairs ware selected. Concerning naturally curly hair, it has been commonly believed that the biased distribution of the paracortex-like structure on the concave side and the orthocortex-like structure on the convex side was related to curl (13). On the other hand, it is known that straight hair possesses the homogenous distribution of two types of cortical cells (13).

The hair samples (15 hairs per specimen) described in the following text were measured using a scanning microbeam SAXS (beamline BL40XU) at the large synchrotron radiation facility SPring-8 (Proposal No. 2012B1388). The temperature and humidity in the facility were 26°C and 30% RH, respectively. The measurement conditions were as follows: X-ray wavelength: 0.083 nm (X-ray energy: 15 keV), camera length: approx. 1612 mm, beam size diameter: approx. Five micrometre (1st pinhole: 5 μm, 2nd pinhole: 200 μm), beam stop diameter: 6 mm, exposure time: 3 s. An imaging intensifier (4 inch) and CCD camera (ORCA-II-ER; Hamamatsu Photonics Co., Ltd., Hamamatsu, Japan) were used as detectors. Calibration was carried out using silver behenate ($d = 5.838$ nm). X-rays were radiated perpendicularly to the fiber axis. The sample position with respect to the X-ray microbeam was moved by steps of 5 μm from the fiber periphery to the center of the fiber. The measurement of the perm-treated hairs started from the convex side of the curl. We then extracted a scattering intensity profile from the two-dimensional SAXS pattern, and simulated the equatorial intensity profile around the scattering vector $S = 0.118$ nm^{-1} to obtain the distance between IFs by using the method proposed by Briki *et al.* (14). Based on the scattering intensity profile in an azimuthal direction around $S = 0.118$ nm^{-1}, the full width at half maximum (FWHM) of the peak derived from IFs was obtained and used as an index of the IF orientation with respect to the hair longitudinal axis (expressed in degrees).

The *t*-test was used to evaluate significant differences in all the statistical analyses (bilateral distribution, $\alpha = 0.05$, $*p < 0.05$, $**p < 0.01$, $***p < 0.001$).

CHEMICAL TREATMENTS FOR SAXS MEASUREMENTS

Bleached hair. Bleached hairs were prepared in the same manner as described previously.

Permed hair. Permed hairs were prepared in the same manner as described previously.

Stretched hairs. The permed hairs were repeatedly stretched 50 times with a force of 0.1 N using a SV-201N type tension/compression testing machine (IMADA SEISAKUSHO Co., Ltd., Toyohashi, Japan) to restore their original state.

SLS immersed hair. The permed hairs were immersed in 5.0 wt% SLS aq. (pH 8.5) for 3 min, 30 times.

Stretched SLS immersed hair. After immersing permed hairs in 5.0 wt% SLS aq. (pH 8.5), the hairs were repeatedly stretched 50 times with a force of 0.1 N using a SV-201N type tension/compression testing machine to restore their original state.

RESULTS

CURL DIAMETER EFFICIENCY

As shown in Figure 1, the phenomenon of curl fallout was validated in the three types of hair samples. Among them, the stretched SLS immersed hair had the lowest value of curl diameter efficiency (82.6%). There was a significant difference between the permed hair and the stretched SLS-immersed hair ($p = 0.007$). The stretched hair (90.8%) or SLS-immersed hair (95.3%) also had lower values of curl diameter efficiency than the permed hair (97.1%).

SAXS MEASUREMENTS

Figure 2 shows a typical 2-D profile measured using SAXS. A strong scattering peak derived from the IFs was observed on the equatorial axis. To examine if the IF's organization

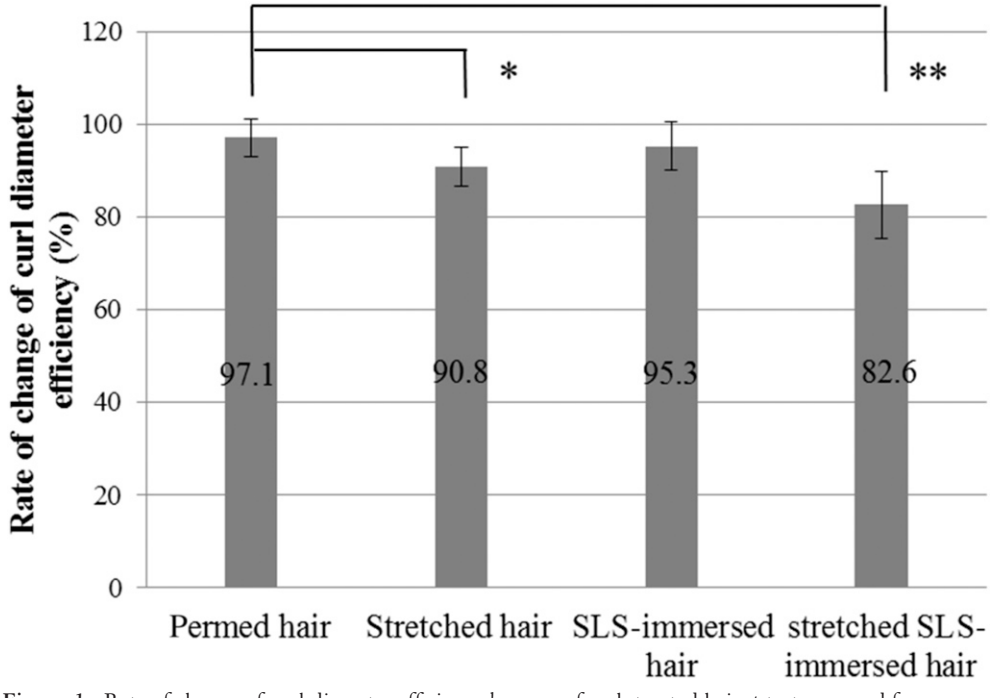

Figure 1. Rate of change of curl diameter efficiency because of each treated hair. *t*-test was used for statistical analysis with $*p < 0.05$, $**p < 0.01$, $***p < 0.001$.

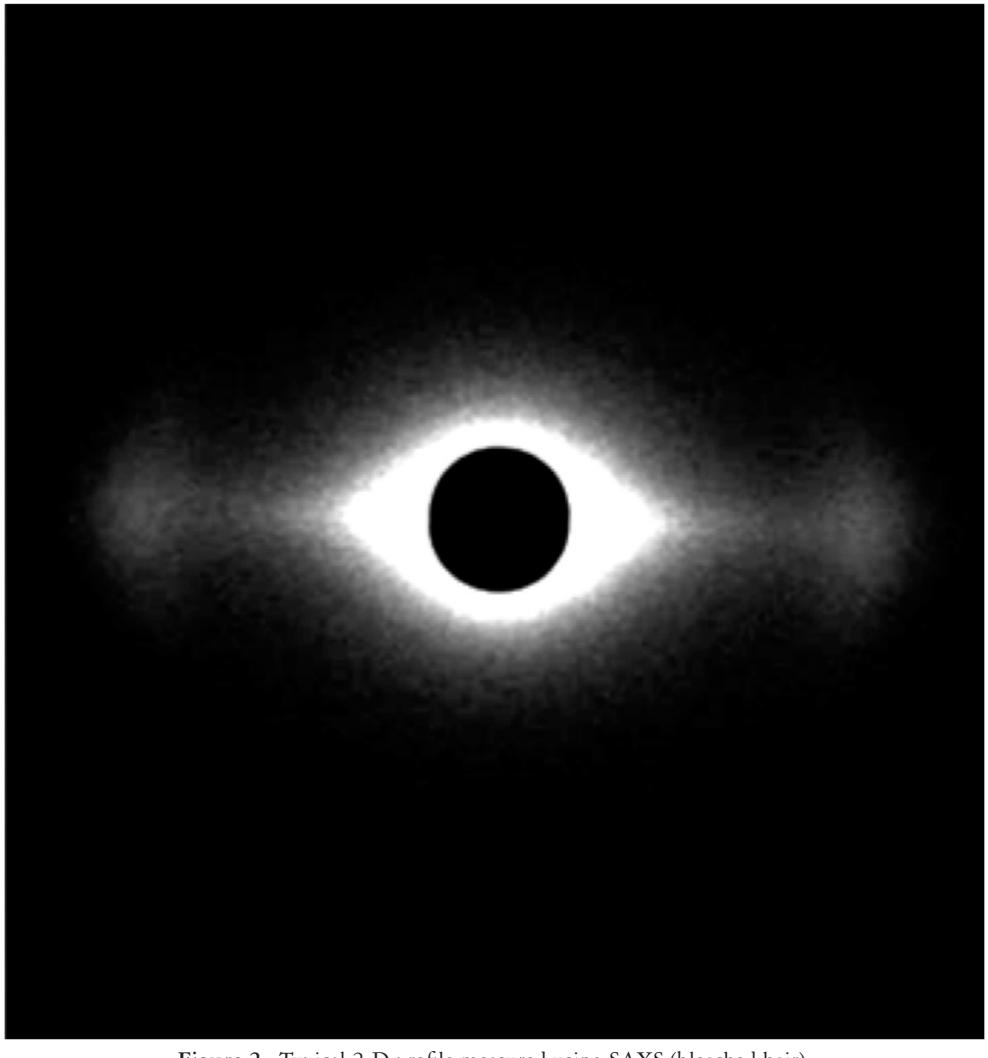

Figure 2. Typical 2-D profile measured using SAXS (bleached hair).

was different in our differently treated hair samples, a scattering intensity profile was extracted from the 2-D profile.

Figure 3 shows typical scattering intensity profiles for four different hair samples. The bleached hairs displayed the highest scattering intensity, followed by the permed hairs, and finally the permed hairs with curl fallout.

The IF organization in the various hair samples was analyzed in detail. The distance between IFs and the FWHM of the scattering intensity profile peak were found to be larger in the permed hairs compared with the bleached hairs (control sample) as is shown in Figure 4. Therefore, we could conclude that the IF orientation of the permed hairs was anisotropic. In addition, it was found that the distance between IFs on the convex side of the hair curvature was different from that on its concave side, and the IFs on the convex side were aligned anisotropically, whereas those on the concave side were aligned isotropically.

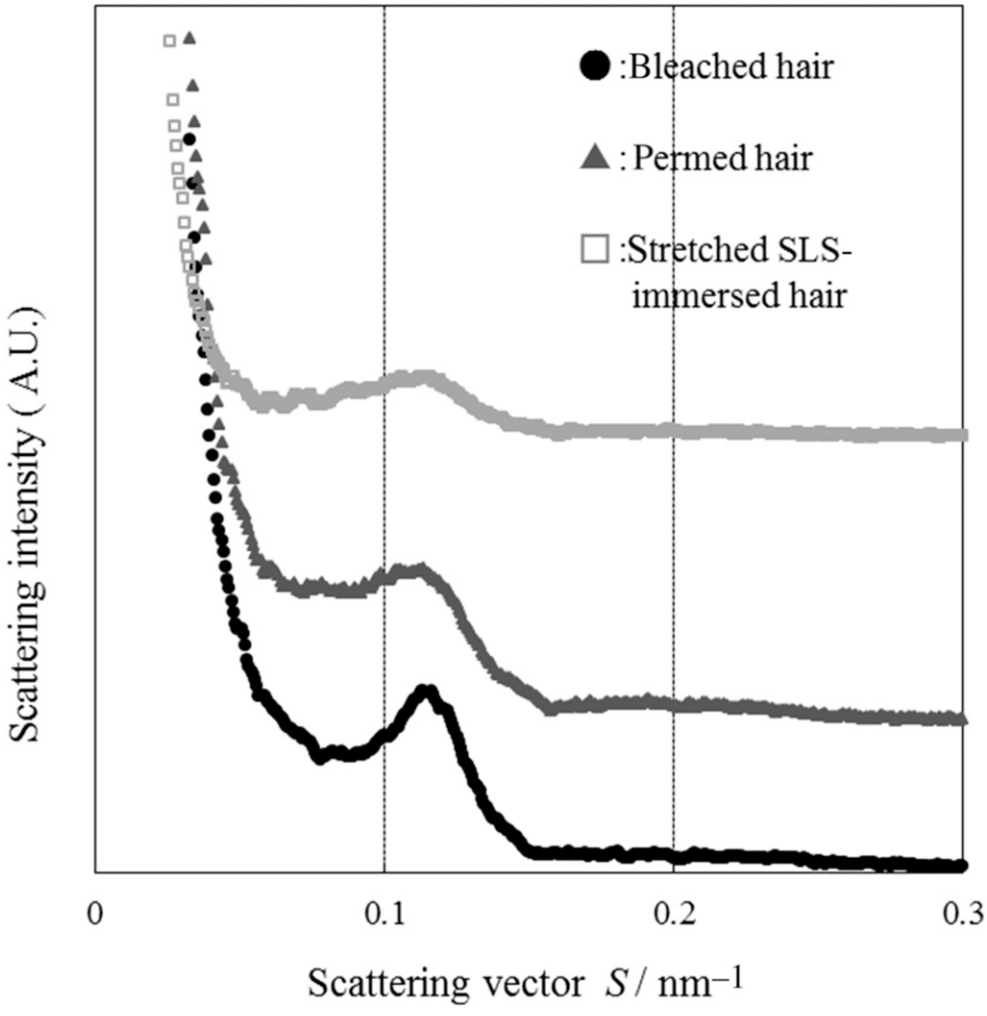

Figure 3. Change of scattering intensity profile extracted from the equatorial axis.

On the other hand, the distance between IFs and the FWHM in the bleached hair were observed in the symmetry with the center of hair shaft as an axis, as expected.

Figure 5 shows the results of the analysis for the permed hair and the stretched hair. Although distance between IFs in the stretched hairs had no difference with that in the permed hairs, the FWHM in the stretched hair was smaller than that in the permed hair.

Figure 6 shows the results of the SLS-immersed hair compared with the permed hair. The distance between IFs and the FWHM in the SLS-immersed hairs was smaller than those in the permed hairs.

Figure 7 shows the results of the stretched SLS-immersed hair compared with the permed hair. Although distance between IFs in the stretched SLS immersed hairs had no difference compared with that in the permed hairs, the FWHM in the stretched SLS immersed hair was smaller than that in the permed hair. Thus, the IF orientation was isotropic for

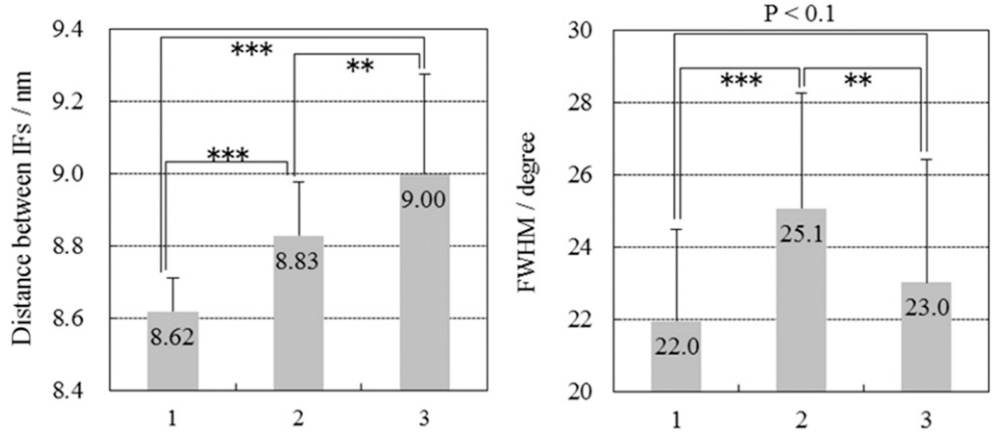

Figure 4. Distance between IFs and FWHM for bleached hair and permed hair. 1: Mean values for the cortex of bleached hair. 2: Mean values for the convex curvature side of permed hair. 3: Mean values for the concave curvature side of permed hair. *t*-test was used for statistical analysis with $*p < 0.05$, $**p < 0.01$, $***p < 0.001$.

the permed hair with these treatments. As a result, the difference in IFs orientation found between the convex and concave side of the stretched SLS-immersed hairs were narrowed.

DISCUSSION

The distance between IFs was found to be larger in permed hair compared with bleached hair. This is believed to be because of changes in intermolecular bonds, including disulfide bonds, due to the chemicals used in perming. Furthermore, on comparing the convex and concave sides of permed hair, the FWHM were found to be significantly larger on the convex side. This is possibly because IFs exist in different orientations on the concave and convex sides, as it is wrapped around the rod. According to previous research on naturally curly hair using SAXS, lack of homogeneity in IF orientation between the convex and concave sides of the curl plays a major role in affecting hair curl morphology (10). In case of permed hair, anisotropic IF orientation between the convex and concave sides of the curl seemed to be similarly related to macroscopic hair curl.

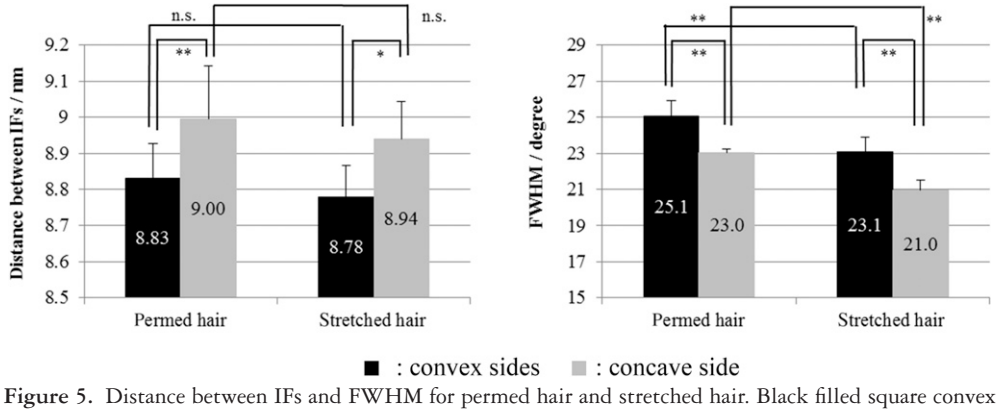

Figure 5. Distance between IFs and FWHM for permed hair and stretched hair. Black filled square convex sides and gray filled square concave side. *t*-test was used for statistical analysis with $*p < 0.05$, $**p < 0.01$, $***p < 0.001$.

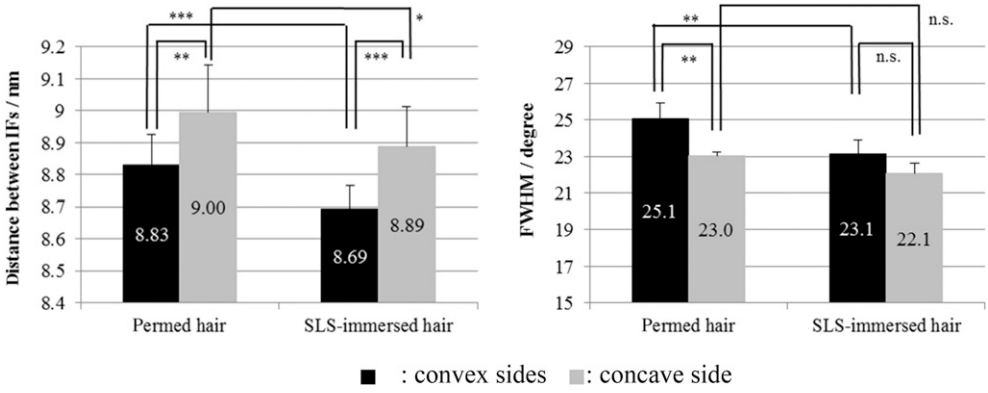

Figure 6. Distance between IFs and FWHM for permed hair and SLS immersed hair. Black filled square convex sides and gray filled square concave side. *t*-test was used for statistical analysis with $*p < 0.05$, $**p < 0.01$, $***p < 0.001$.

It was observed that curl diameter efficiency of the stretched hair, SLS-immersed hair, and stretched SLS-immersed hair was significantly lower than that of permed hair. Therefore, the changes in microstructure that occur when a permed curl falls out are discussed.

First, stretched hair was compared with permed hair. No differences were present in the distances between IFs, whereas FWHM of stretched hair was significantly smaller than that of permed hair. A previous study reported that the sliding of keratin molecule along the IF axis when the hair was stretched (15). It was considered that the stretched treatment affected leading IF orientation by causing it to become isotropic.

Subsequently, comparison of SLS-immersed hair and permed hair revealed that the distance between IFs in SLS-immersed hair was significantly smaller than that of permed hair. In addition, FWHM in the convex side of the curl in SLS-immersed hair was significantly smaller than that in permed hair. Therefore, SLS immersion affected leading IF orientation by causing it to become isotropic. Concerning the distance between IFs, it was thought a possibility that the flow-out or swelling of Intermediate filament associated protein (IFAP) occurred in SLS immersion. Concerning the FWHM, a hypothesis was substantiated; in

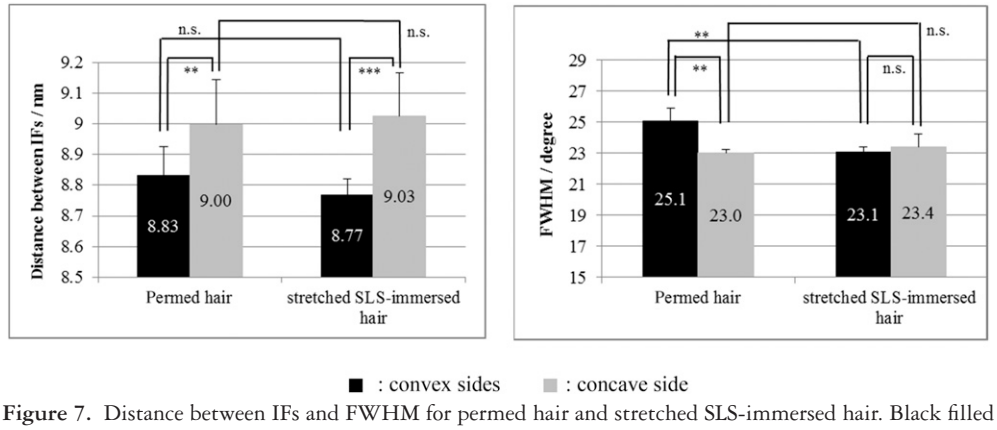

Figure 7. Distance between IFs and FWHM for permed hair and stretched SLS-immersed hair. Black filled square convex sides and gray filled square concave side. *t*-test was used for statistical analysis with $*p < 0.05$, $**p < 0.01$, $***p < 0.001$.

case of inclined IFs as seen in the orthocortex (12), swelling of IFAP longitudinally aligned the slope of the IFs, which led to the IF orientation becoming isotropic.

Last, in the comparison of stretched SLS-immersed hair and permed hair, there were no differences in distance between IFs, whereas FWHM in the convex side of the curl in stretched SLS-immersed hair was significantly smaller than that of the permed hair. Responsiveness on the convex side of the curl was more noticeable because of the difference in the stretching strain between the convex and concave sides of the curl when making the curl shapes (16). Therefore, it was conjectured that the change in the convex side was more noticeable when the strain was relieved. According to previous research, it was reported that IF orientation in straight hair was isotropic (12), and isotropic IF orientation was related to macroscopic hair straightening (10). Our research similarly clarified that the macroscopic curl fallout of permed hair was related to an isotropic IF orientation between the convex and concave sides of the curl.

CONCLUSIONS

Using microbeam SAXS measurements to change the shape of permed hair, it was clarified that IF orientation plays a major role in hair morphology; anisotropic IF orientation between the convex and concave sides of the curl are related to curl shape. On the contrary, isotropic IF orientation between the convex and concave sides of the curl correlated with the macroscopic curl fallout.

It was found that stretching and SLS immersion leads to isotropic of IF orientation. Furthermore, a combination of both treatments narrows the difference in the IF orientation between the convex and concave sides of the curl. It is hoped that maintenance of anisotropic IF orientation between the convex and concave sides of the curl will allow for effective amelioration of curl fallout.

REFERENCES

(1) S. Naito and K. Arai, Type and location of SS linkages in human hair and their relation to fiber properties in water, *J. Appl. Polym. Sci.*, **61**, 2113–2118 (1996).
(2) S. Ogawa, Y. Takeda, K. Kaneyama, K. Joko, and K. Arai, Characterization of permanent wave and straight hair using high pressure differential scanning calorimetry, *Sen'i Gakkaishi*, **65**(1), 24–33 (2009).
(3) A. Kuzuhara, Analysis of structural change in keratin fibers resulting from chemical treatments using Raman spectroscopy, *Biopolymers*, **77**, 335–344 (2005).
(4) N. Nishikawa, Y. Tanizawa, S. Tanaka, Y. Horiguchi, and T. Asakura, Structural change of keratin protein in human hair by permanent waving treatment, *Polymer*, **39**(16), 3835–3840 (1998).
(5) F. J. Wortmann, C. Popescu, and G. Sendelbach, Effects of reduction on the denaturation kinetics of human hair, *Biopolymers*, **89**(7), 600–605 (2008).
(6) R. D. B. Fraser, T. P. MacRae, and E. Suzuki, Structure of the α-keratin microfibril, *J. Mol. Biol.*, **108**, 435–452 (1976).
(7) M. E. Rafik, J. Doucet, and F. Briki, The intermediate filament architecture as determined by X-ray diffraction modeling of hard α-keratin, *Biophys. J.*, **86**, 3893–3904 (2004).
(8) K. C. Littrell, J. M. Gallas, G. W. Zajac, and P. Thiyagarajan, Structural studies of bleached melanin by synchrotron small-angle X-ray scattering, *Photochem. Photobiol.*, **77**, 115–120 (2003).
(9) N. Ohta, T. Oka, K. Inoue, N. Yagi, S. Kato, and I. Hatta, Structural analysis of cell membrane complex of a hair fibre by micro-beam X-ray diffraction, *J. Appl. Cryst.*, **38**, 274–279 (2005).
(10) M. Kakizawa, T. Kawasoe, N. Ohta, K. Inoue, N. Yagi, and I. Hatta, Small-angle X-ray diffraction structural analysis of human hairs of different shapes and effect of straight perming, *J. Jpn. Cosmet. Sci. Soc.*, **34**, 102–107 (2010).

(11) Y. Kajiura, S. Watanabe, T. Itou, A. Iida, Y. Shinohara, and Y. Amemiya, Structural analysis of single wool fibre by scanning microbeam SAXS, *J. Appl. Cryst.*, **38**, 420–425 (2005).
(12) Y. Kajiura, S. Watanabe, T. Itou, K. Nakamura, A. Iida, K. Inoue, N. Yagi, Y. Shinohara, and Y. Amemiya, Structural analysis of human hair single fibers by scanning microbeam SAXS, *J. Struct. Biol.*, **155**, 438–444 (2006).
(13) W. G. Bryson, D. P. Harland, J. P. Caldwell, J. A. Vernon, R. J. Walls, J. L. Woods, S. Nagase, T. Itou, and K. Koike, Cortical cell types and intermediate filament arrangements correlate with fiber curvature in Japanese human hair, *J. Struct. Biol.*, **166**, 46–58 (2009).
(14) F. Briki, B. Busson, and J. Doucet, Organization of macrofibrils in keratin fibers studied by X-ray scattering modeling using the paracrystal concept, *Biochim. Biophys. Acta.*, **1429**, 57–68 (1998).
(15) L. Kreplak, A. Franbourg, F. Briki, F. Leroy, D. Dalle, and J. Doucet, A new deformation model of hard α-keratin fiber at the nanometer scale: implications for hard α-keratin intermediate filament mechanical properties, *Biophys. J.*, **82**, 2265–2274 (2002).
(16) T. Kawai, T. Inoue, T. Fujimori, K. Takehara, A. Takeuchi, K. Uesugi, and Y. Suzuki, Imaging of photo-damaged hair with a differential phase scanning X-ray microscopy, *J. Soc. Cosmet. Chem. Jpn.*, **51**(3), 231–236 (2017).